UC Berkeley
UC Berkeley Previously Published Works

Title

A pattern recognition method for electronic noses based on an olfactory neural network

Permalink

https://escholarship.org/uc/item/9tr82425

Journal

Sensors and Actuators B, 125

Authors

Fu, Jun
Li, Guang
Qin, Yuqi
et al.

Publication Date

2007

Peer reviewed

A pattern recognition method for electronic noses based on an olfactory neural network

Jun Fu [a], Guang Li [b,*], Yuqi Qin [a], Walter J. Freeman [c]

[a] *Department of Biomedical Engineering, Zhejiang University, Hangzhou 310027, China*
[b] *National Laboratory of Industrial Control Technology, Zhejiang University, Hangzhou 310027, China*
[c] *Division of Neurobiology, University of California at Berkeley, LSA 142, Berkeley, CA 94720-3200, USA*

Abstract

Artificial neural networks (ANNs) are generally considered as the most promising pattern recognition method to process the signals from a chemical sensor array of electronic noses, which makes the system more bionics. This paper presents a chaotic neural network entitled KIII, which modeled olfactory systems, applied to an electronic nose to discriminate six typical volatile organic compounds (VOCs) in Chinese rice wines. Thirty-two-dimensional feature vectors of a sensor array consisting of eight sensors, in which four features were extracted from the transient response of each TGS sensor, were input into the KIII network to investigate its generalization capability for concentration influence elimination and sensor drift counteraction. In comparison with the conventional back propagation trained neural network (BP-NN), experimental results show that the KIII network has a good performance in classification of these VOCs of different concentrations and even for the data obtained 1 month later than the training set. Its robust generalization capability is suitable for electronic nose applications to reduce the influence of concentration and sensor drift.

© 2007 Published by Elsevier B.V.

Keywords: Artificial neural networks; Electronic nose; Pattern recognition; Transient phase; Olfactory model; Sensor drift

1. Introduction

The molecular basis of odor recognition in the human olfactory system has been successfully investigated [1], while the information processing principle of olfactory neural systems still remains not very clear. However, a bionic technology termed electronic noses inspired by the mechanism of biological olfactory systems has been studied by many researchers during the past two decades [2]. An electronic nose is an instrument, which generally consists of an array of cross-sensitive electronic chemical sensors and an appropriate pattern recognition method (PARC), to automatically detect and discriminate simple or complex odors [3]. Generally speaking, electronic noses are faster to respond, easier to use and relatively cheaper in comparison with conventional analytical techniques, such as gas chromatography/mass spectroscopy (GC/MS) and flame ionization detection (FID), so that they have wide applications in environmental monitoring [4,5], food and beverage industry [6–8], medical diagnosis [9], public security [10], etc.

As a multidisciplinary research, most studies on electronic noses focused on the sensitivities of the chemical sensor array and the pattern recognition methods to process the signals obtained from the sensor array. With the development of functional material technology, signals can be obtained via various sensors, such as metal oxide semiconductor (MOS), optical, conducting polymer (CP), quartz crystal microbalance (QCM) and surface acoustic wave (SAW) sensors [11,12]. However, how to deal with these signals is still crucial for artificial olfaction to reliably recognize various odors. So far, a considerable number of pattern recognition methods have been introduced into electronic noses [13,14]. And ANNs are usually considered to be one of the most promising methods to solve this complicated problem, because they can cope with nonlinear problems and handle noise or drift better than conventional statistical approaches. So many ANNs to process signals from sensor arrays are reported, such as back propagation trained neural network [15], radial basis function neural network [16], probabilistic neural network [17], self-organizing network [18], etc.

* Corresponding author. Tel.: +86 571 87952233 8228.
E-mail address: guangli@zju.edu.cn (G. Li).

Although conventional ANNs simulate the hierarchy structure of cortex, only a few of ANNs mimic the architectures of a particular neural system. Multi-scale models entitled K sets were introduced by Freeman in the 70′, which described increasing complexity of structure and dynamical behaviors. K-sets are topological specifications of the hierarchy of connectivity in neuron populations, and the KIII network is a complex dynamics system to imitate vertebrate olfactory systems [19,20]. When the parameters are optimized and additive noise is introduced, the KIII network can not only output electroencephalograph-like waveforms observed in electrophysiological experiments [21–23], but also be used in a wide range of applications, including spatiotemporal EEG pattern classification [24,25] and handwritten numerals recognition [26]. Recently, Gutierrez-Osuna and Gutierrez-Galvez have shown the potential use of the KIII network to analyze the output signal of a chemical sensor array [27]. They also proposed a new Hebbian/anti-Hebbian learning rule for this model to increase pattern separability for different concentrations of three VOCs [28].

Focusing on the problems of concentration influence and sensor drift, this paper reports an application of the KIII neural network on an electronic nose to recognize VOCs usually present in the headspace of Chinese rice wine.

2. Experimental

2.1. Experimental setup and data acquisition

The experimental setup consists of an array of eight MOS sensors in a sealed test chamber (3000 mL), a set of acquisition circuits including a 12-bit A/D converter and an IBM PC compatible computer (as shown in Fig. 1). The communication between the signal acquisition circuits and the computer is via a RS232 cable. Eight sensors (TGS880 (2×), TGS813 (2×), TGS822 (2×), TGS800, TGS823) are all commercially available, purchased from Figaro Engineering Inc.

Six VOCs (ethanol, acetic acid, acetaldehyde, ethyl acetate, lactic acid and isoamyl alcohol) usually presenting in the headspace of Chinese rice wines [29] were of analytical grade and purchased from Sinopharm Chemical Reagent (Shanghai, China). For each VOC, 10 mL solution was rested on the bottom of a 250 mL vial at least 20 min, so that saturated VOC could be extracted in the headspace of the vial as an analyte.
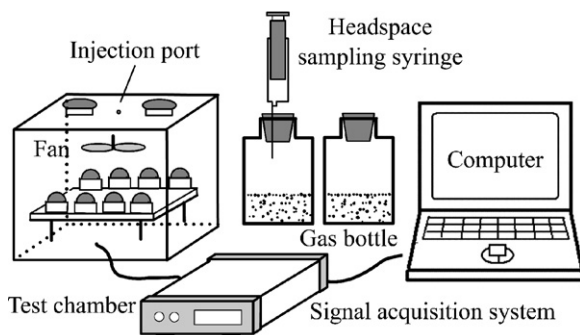

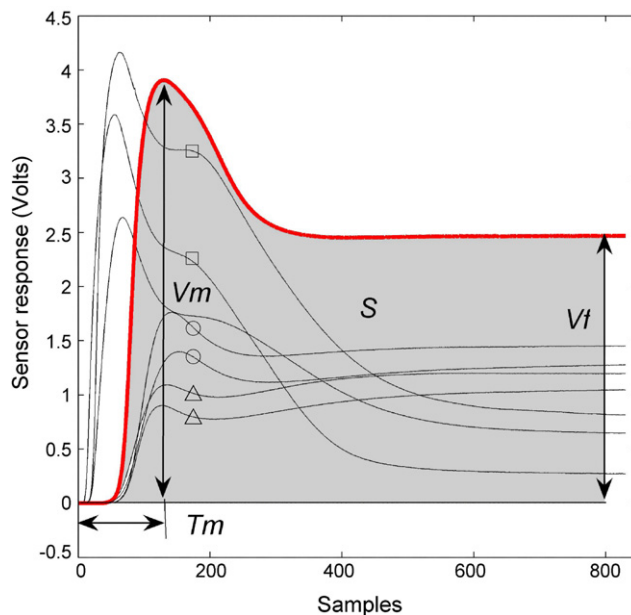
Fig. 1. Scheme of the experimental setup.

Fig. 2. A typical output of the sensor array. Features extracted from the response of one sensor are indicated as V_m, T_m, V_f and S. The curves marked with the same symbol ($\square$, $\bigcirc$ and $\triangle$) were obtained from the same type sensors.

To distribute the analyte uniformly in the test chamber, a fan inside the chamber stirred air for 1 min after the VOC was extracted from the vial headspace and then injected into the test chamber using a syringe. When a constant voltage (5 V dc) was applied to the heater resistors of all sensors, the outputs of eight sensors were simultaneously measured via the 12-bit 8-channel A/D converter and recorded on the hard disk of the PC for further processing. The sampling rate for each sensor was 20 samples/s and the duration was 1 min. Fig. 2 shows typical response curves of the sensor array. The same type of sensors have similar but not the same response characteristics, as shown in Fig. 2, implying that no one is redundant. After measurement, the test chamber was flushed with ambient airflow for 5 min to purge the chamber and leave the sensors to recover by desorption. All measurements were carried out under open laboratory conditions without special atmospheric, humidity or temperature control.

In order to investigate the sensor drift effect, data acquisition were conducted during different periods. Dataset I was collected in May, containing 66 samples (11 samples for each of six VOCs), and Dataset II was collected in June, containing 120 samples (20 samples for each of six VOCs). All the concentrations of VOCs for Datasets I and II are 30 mL/3000 mL. Dataset III was acquired in August, containing 90 samples (five samples for each of six VOCs of 30 mL/3000 mL, 50 mL/3000 mL and 70 mL/3000 mL concentrations).

2.2. Feature extraction

A typical output of the sensor array consists of eight time series from eight individual sensors. Some features should be extracted to represent the original signals for further processing. Many feature extraction methods have been considered, includ-

ing steady-state phase, transient phase or both. However, it is commonly believed that the transient response, which represents different dynamic behaviors of the sensors exposed to different odors [30], may contain more information than steady-state one. Besides, utilizing transient response reduces the time requirement to collect data. In this work, four features were selected (as shown in Fig. 2) to construct a feature vector to represent one response of the sensor array to a certain VOC; (1) the maximum voltage of sensor output, V_m, (2) the time to reach the maximum voltage, T_m, (3) the voltage at 40 s, V_f, and (4) the area covered by the response curve during the first 40 s, S, which is estimated as the sum of the data values of the first 40 s.

In order to reduce the influence of concentration fluctuation on classification results, a vector normalization is applied as described in Eq. (1). Each set of vector is individually divided by its Euclidean norm so that it lies in a hyper-sphere of unit radius.

$$P_{new}(i) = \frac{P(i)}{\left(\sum_{i=1}^{8} P^2(i)\right)^{1/2}}, \quad i = 1, 2, ..., 8 \tag{1}$$

where $P(i)$ represents V_m, T_m, V_f and S, respectively. Eq. (1) is given for each feature from the eight sensors. Therefore, the response of the sensor array to a certain VOC can be represented by a 32-dimensional feature vector.

3. Pattern recognition method

3.1. KIII neural network

The KIII network modeling biological olfactory systems is a massively parallel architecture with multiple layers coupled with both feedforward and feedback loops through distributed delay lines. Fig. 3 shows the topological diagram of the KIII network. Odorant sensory signals from receptors (R) propagate to periglomerular cells (P) and olfactory bulb (OB) layers via the primary olfactory nerve (PON) in parallel. The OB layer consists of a set of mutually coupled neural oscillators, each being formed by two mitral cells (M) and two granule cells (G). Then the sum output of all lateral M1 nodes transmits via a lateral olfactory tract (LOT) to the AON and PC, which provides the final output of the olfactory system to other parts of the brain from deep pyramidal cells (C), as well as back to the OB and AON layers. Details of the KIII network and its neurophysiologic foundations are given in Refs. [19,21,23,31,32].

In Fig. 3, every node representing a population of interactive neurons can be described by a second-order ordinary differential equation (ODE) as follows:

$$\frac{1}{ab}[x_i''(t) + (a+b)x_i'(t) + abx_i(t)]$$

$$= \sum_{j\neq i}^{N} \left[W_{ij}Q(x_j(t), q_j)\right] + I_i(t) \tag{2}$$

where $x_i(t)$ represents the state variable of the ith node, $x_j(t)$ represents the state variable of the jth node, which is connected to the ith, while W_{ij} indicates the connection strength from j to i. $I_i(t)$
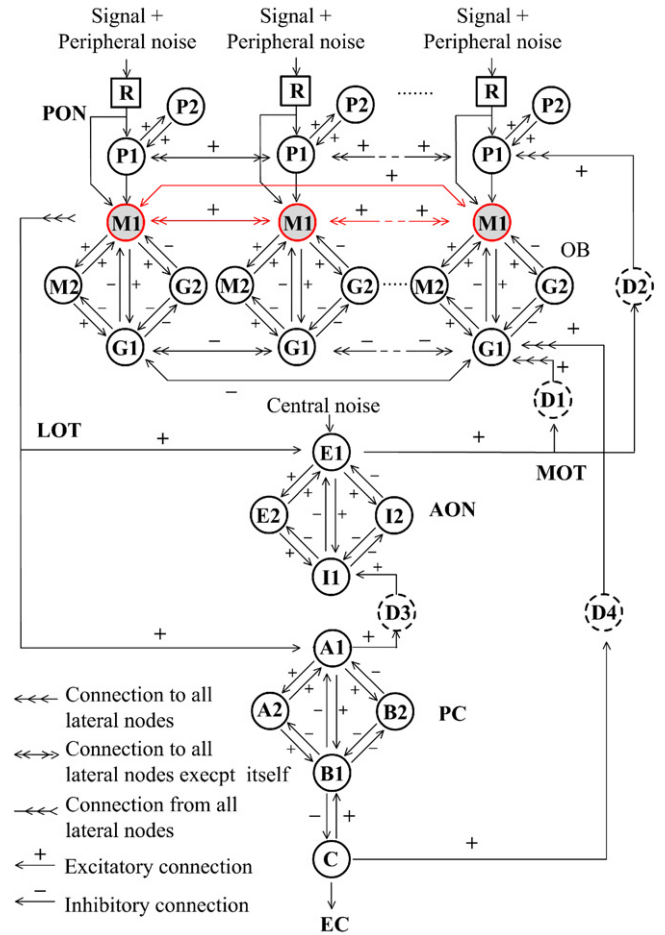

Fig. 3. Topology of the KIII neural network.

is an external input signal to the ith node. The parameters a and b reflect two rate constants. $Q(x(t), q)$ is a static sigmoid function derived from the Hodgkin-Huxley equation and evaluated by experiments [33].

$$Q(x(t), q) = \begin{cases} q(1 - \exp(-(\exp(x(t)) - 1)/q)), & x(t) > -x_0 \\ -1, & x(t) \leq -x_0 \end{cases}$$

$$x_0 = -\ln\left(1 - q\ln\left(1 + \frac{1}{q}\right)\right) \tag{3}$$

Therefore, the dynamics of the whole olfactory model can be mathematically described by a set of such ODEs, as details in Refs. [19,22]. Here, the fourth-order Runge-Kutta method with a fixed step of 1 was applied for numerical integration of the ODEs.

The parameters in the model are determined by a set of reliable parameter optimization algorithms [21] to make the KIII model output EEG-like waveform as observed in olfactory systems. All parameters without declaration in this paper come from Ref. [22]. Moreover, it seems to be very important to introduce additive noises into the KIII network for its stability and robustness. Therefore, a low-level Gaussian noise is injected into two significant points, R and AON to simulate both peripheral and
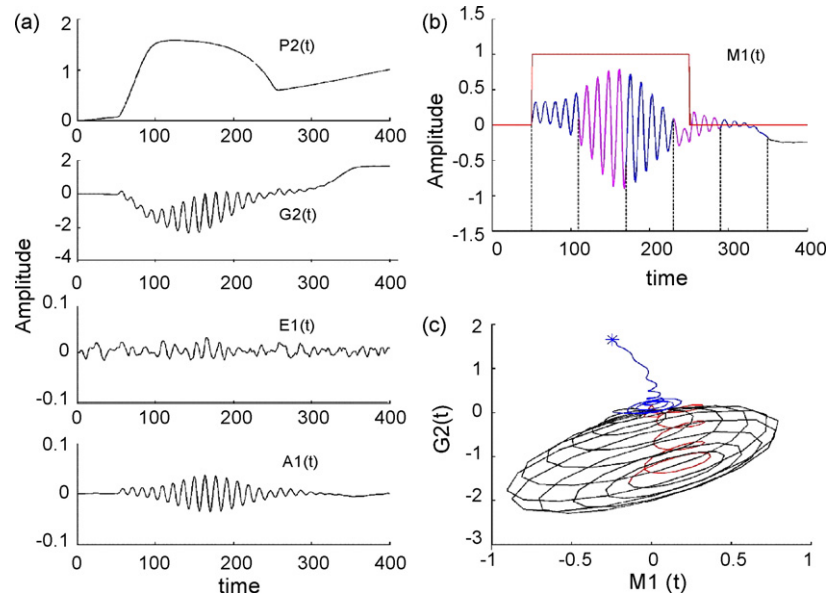
Fig. 4. An example of time series from (a) P2, G2, E1, A1 and (b) M1 node of the 32-channel KIII network with constant stimulus from 50 to 250 steps injected via receptor. (c) The phase portrait of attractor with M1 node against G2 node in OB (start from red, then to black and end in blue) (For interpretation of the references to colour in this figure legend, the reader is referred to the web version of the article.).

central sources of noise in olfactory systems. It offers a convergence of statistical measures on the KIII output trajectories under perturbations of initial conditions of variables and parameter values [22].

3.2. Learning rule and classification algorithm

When a pattern to be learned expressed by an n-dimension vector is input in parallel into an n-channel KIII network, the system that presents an aperiodic oscillation in its basal state at first will soon go to a specific local basin of an attractor wing, with a gamma range of quasi-periodic burst, corresponding to this pattern, as shown in Fig. 4. The system memory is defined as the collection of basins and attractor wings of the KIII network, and a recall is the induction by a state transition of a spatiotemporal gamma oscillation [24]. When used for pattern recognition, the outputs of the KIII network are expressed in the form of a spatial amplitude modulated (AM) pattern of a chaotic oscillation in the multi-channel OB layer. Many mathematical methods to extract information from the outputs of the model are proposed, such as standard deviation (SD) [24], singular-value decompositions (SVD) [34], root mean square (RMS), principal components analysis (PCA) and fast Fourier transform (FFT) [35].

In this work, the SD method is adopted. The burst in each M1 node is portioned into s equal segments, and the mean value of the individual SD of these segments is calculated as SD(k), as in Eq. (4).

$$SD(k) = \frac{1}{s}\sum_{r=1}^{s}SD_r, \quad k = 1, 2, ..., n \tag{4}$$

When a new sample is presented to the KIII network with n channels, the activity measure over the whole OB layer in this

training can be expressed by a vector:

$$\Phi = [SD(1), SD(2), \ldots, SD(n)] \tag{5}$$

In training phase, every time the modified Hebbian learning rule and the habituation learning rule [24] are employed to modify lateral weights W_{mml} between all M1 nodes in the OB layer (short for W_{ij} and W_{ji}), as shown in Eq. (6). If the activities of two nodes, M1(i) and M1(j) for each pair of i and j, are larger than the mean activity of the OB layer, they are considered to be co-activated by the external stimulus and their connection weights are strengthened by the modified Hebbian learning rule. Otherwise their connection weights decrease at the habituation rate h_{hab} and eventually diminish asymptotically toward zero after several learning cycles.

IF $SD(i) > (1 + K)SD_m$ AND $SD(j) > (1 + K)SD_m$

THEN $W'_{ij} = h_{Heb}$, $W'_{ji} = h_{Heb}$ (6)

ELSE $W'_{ij} = h_{hab}W_{ij}$, $W'_{ji} = h_{hab}W_{ji}$

where $SD_m = (1/n)\sum_{k=1}^{n}SD(k)$ and $i, j, k = 1, 2, \ldots, n$ and $i \neq j$. W' stands for the weight after learning, while W is the original weight; h_{Heb} and h_{hab} are the learning constant of the Hebbian reinforcement and habituation, respectively. The bias coefficient K is defined to avoid the saturation of the weight space.

The learning process continues until the weight changes of W_{mml} converge to a desired level. At the end of learning, the cluster centroid of every pattern C_i is determined and the connection weights are fixed in order to perform classification using the trained network. While inputting an unknown sample t from the test set, the Euclidean distances from the corresponding activity vector Φ_t to those training pattern cluster centroids C_i are estimated, and the minimum distance determines the classification.

All calculations and data processing in this study were implemented in MATLAB (version 7.1, Mathworks, USA) on a

Dell Pentium-4 personal computer (CPU 3.00 GHz and RAM 1.00 GB, Dell Inc., USA) running Windows XP (Mircosoft, USA).

4. Results and discussion

4.1. KIII neural network implementation

Each simulation of a trial for either training or testing lasts about 400 steps. The first 50 steps is the initial period in which the KIII network enters its basal state, and the input is on during 50–250 steps. In the last 150 steps, the KIII network goes back to the initial state. All output information of the KIII network are observed from M1 nodes in the OB layer, and the burst between 50 and 350 steps in each M1 is equally partitioned into five segments, as shown in Fig. 4(b). The parameters mentioned in Section 3.2 are $h_{Heb} = 0.0395$, $h_{hab} = 0.8607$ and $K = 0.4$, which are determined empirically.

Firstly, how the weight matrices of *Wmml* converge with the learning cycle number is studied to determine how many learning cycles are needed. The Dataset I is used to train the KIII network. The KIII network is trained 10 cycles alternately with VOCs' feature vectors. The overall weight change, $\Delta Wmml$, indicated by the sum of square of each weight change, is shown in Fig. 5. It can be seen that $\Delta Wmml$ descends rapidly with an increase of the number of learning cycles. When a threshold of the weight change is fixed, the number of the learning cycles needed can be easily determined. An example is shown in Fig. 5. In our experiments, the number of learning cycles is between four and six, which guarantees $\Delta Wmml$ in the order of 10^{-4}.

Dataset I, containing 66 samples (11 samples for each of six VOCs), was used here to investigate the general performance of the KIII network. Trained with one of the samples of each
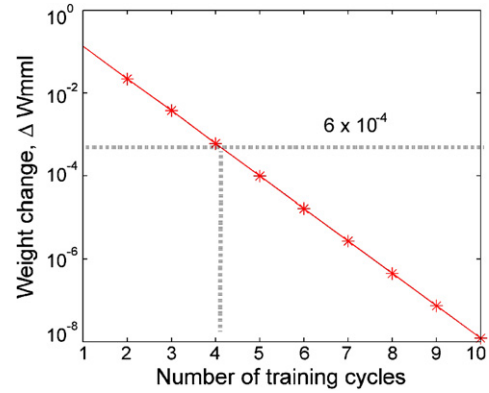

Fig. 5. Convergence curve of the overall weight change, $\Delta Wmml$, with respect to the number of learning cycles in a semi-log plot. The number of training cycles can be easily determined by the threshold (e.g., 6×10^{-4}).

of six VOCs, the Euclidean distances of all samples, including the training set, to different cluster centroids of those six classes are shown in Fig. 6. According to the classification criteria described in Section 3.2, the classification results clearly show that the correction rate of most samples are close to 100%, except two samples were misclassified. Two lactic acid samples were misrecognized as acetic acid (as shown in Fig. 6(a)), while another sample of acetic acid was misrecognized as lactic acid (as shown in Fig. 6(c)). In each subplot, the Euclidean distance of the first VOC sample to its own cluster centroid is usually the smallest, since the sample was used to train the KIII.

4.2. Concentration influence elimination by the KIII

A challenge of electronic nose applications is the pattern dispersion caused by concentration difference. Most work to
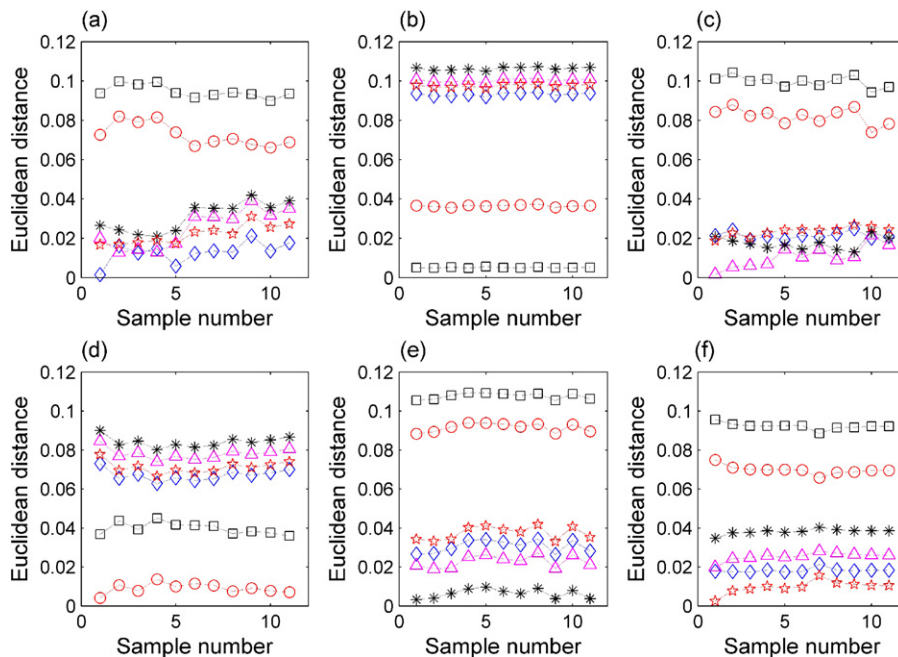

Fig. 6. Euclidean distance from all samples in Dataset I to different cluster centroids of: (a) lactic acid, (b) ethanol, (c) acetic acid, (d) ethyl acetate, (e) isoamyl alcohol and (f) acetaldehyde. Symbols: (◊) lactic acid, (□) ethanol, (△) acetic acid, (○) ethyl acetate, (*) isoamyl alcohol and (☆) acetaldehyde.

Table 1
Correction rate of classification (%) of the KIII trained by 30 mL/3000 mL, 50 mL/3000 mL and 70 mL/3000 mL samples, respectively

	30 mL/3000 mL	50 mL/3000 mL	70 mL/3000 mL
Lactic acid	100	100	100
Ethanol	50.0	100	66.7
Acetic acid	100	91.7	75.0
Ethyl acetate	100	100	100
Isoamyl alcohol	75.0	100	100
Acetaldehyde	100	100	100
Average	87.5	98.6	90.3

eliminate this influence concentrated on applying different normalization methods to preprocess the data. However, linear normalization methods like Eq. (1) only work in a small scale of concentration fluctuation because most sensor responses are logarithmically dependent on gas concentration. In other words, for nonlinear sensors this normalization does not cancel the concentration dependence completely. An efficient algorithm for an electronic nose should identify chemicals independently of their concentrations. And ANNs seem one of the appropriate algorithms. Here Dataset III was used to test the KIII network to eliminate the concentration influence.

Three samples with the same concentration were randomly chosen to train the KIII network, while the others in Dataset III were used for testing. Classification results of the KIII trained by different concentrations (30 mL/3000 mL, 50 mL/3000 mL and 70 mL/3000 mL) are shown in Table 1. The average classification accuracy of the KIII network trained by 50 mL/3000 mL samples is 98.6%, which is higher than those by 30 mL/3000 mL and 70 mL/3000 mL. It is reasonable because the pattern normally varies from one to another gradually as the concentration changes and 50 mL/3000 mL is in the middle of the concentration gradient. No matter which concentration is used to train, a correction rate better than 87% is achieved. In other words, the concentration error tolerance in a span of 40 mL/3000 mL should be about 87%. Although it may be not good enough in comparison with biological olfaction, this concentration tolerance may meet some application requirements when the data acquisition conditions are strictly controlled.

4.3. Sensor drift counteraction by the KIII

Another key issue for an electronic nose is that the chemical sensors tend to show significant variations over long time periods when exposed to identical atmospheres. These so-called sensor drifts are due to the aging of the sensors, poisoning effects, and perhaps fluctuations in the sensor temperature because of environmental changes [36]. It is very important for an electronic nose to have robust generalization and error tolerance capability in order to avoid the regular requirement of sensor calibration or ANN retraining before each use. The need to deal with the sensor drift of electronic noses has been long recognized and various strategies [36,37] have been developed to solve this problem. The following experiments were addressed to investigate the drift counteraction capability of the KIII network.
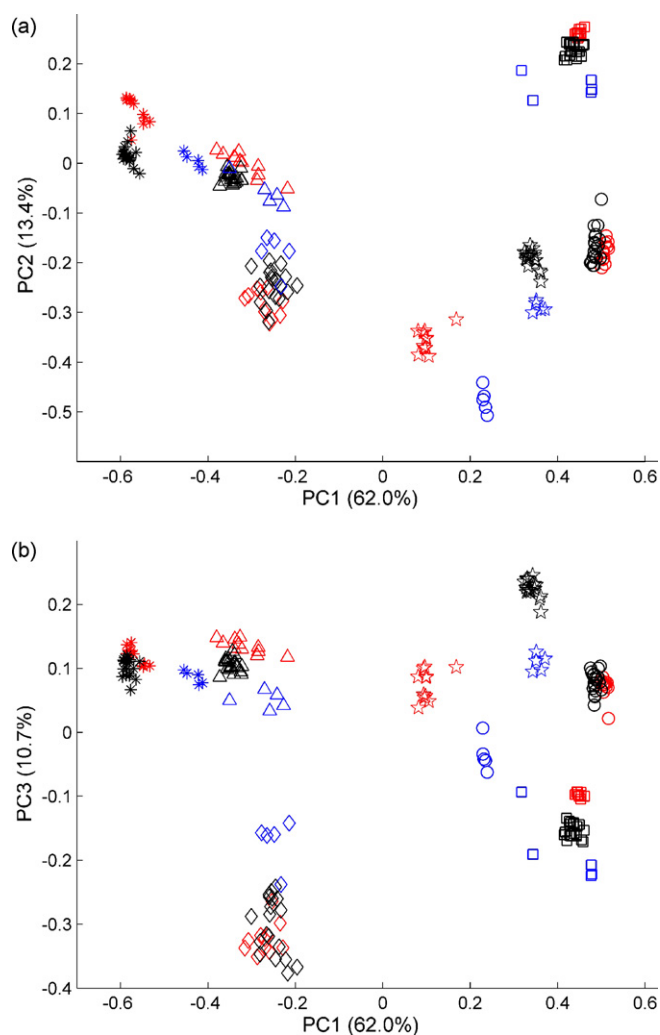

Fig. 7. PCA plots of six VOCs collected in May (Dataset I, red), June (Dataset II, black) and August (Dataset III, blue). Symbols: (◇) lactic acid, (□) ethanol, (△) acetic acid, (○) ethyl acetate, (*) isoamyl alcohol and (☆) acetaldehyde.

A dimension reduction technique, PCA, can help to get a better understanding of the nature of sensor drifts, through giving an appropriate visual representation of the raw data with fewer dimensions. Fig. 7 illustrates the PCA plots, which show the difference between Datas I, II and III, obtained in May (red), June (black) and August (blue), respectively. Different VOCs are represented by different symbols. Examining these PCA plots, the first three principal components accounted for 86.1% of the variance of the data. The clustering of different VOC samples from one dataset (samples collected during the same time period) is obvious. However, some sensor drifts occurred significantly, for examples the acetaldehyde (☆) samples in June and August are far away from those in May, the ethyl acetate (○) samples being the same.

The KIII network was trained with six samples, corresponding to six kinds of VOCs, chosen from Dataset I. Then the procedure, in which other samples in Dataset I, all samples in Dataset II and the samples with a concentration of 30 mL/3000 mL in Dataset III were classified by the trained network, was considered as one trial. The average correction rates

Table 2
Classification correction rates (%) of Datasets I, II and III using the KIII, NPA and BP-NN

	Dataset I (May)			Dataset II (June)			Dataset III[a] (August)		
	KIII	NPA	BP-NN	KIII	NPA	BP-NN	KIII	NPA	BP-NN
Lactic acid	85.0	100	87.7	98.0	100	78.3	50.0	83.3	48.6
Ethanol	100	100	100	100	100	87.6	100	100	62.0
Acetic acid	100	100	86.3	100	100	74.5	86.7	100	52.6
Ethyl acetate	100	100	100	100	100	99.3	0	0	44.6
Isoamyl alcohol	100	100	97.3	100	100	86.5	86.7	93.3	52.0
Acetaldehyde	100	100	86.0	65.0	0	18.3	46.7	0	28.7
Average	97.5	100	92.9	93.9	83.3	74.1	61.6	62.7	48.1

[a] Only the samples with concentration of 30 mL/3000 mL in Dataset III are used to make the results comparable with Datasets I and II.

of six trials are shown in Table 2. For the KIII network, the average correction rates for the samples of Datasets I, II and III are 97.5%, 93.9% and 61.6%, respectively. It is clear that the classification accuracy declined a little 1 month later though it dropped dramatically 3 months later. It can be seen that the KIII network has capability to counteract the sensor drift in 1 month. It is not surprising that the KIII network misrecognized all ethyl acetate as acetaldehyde in Dataset III since the samples of ethyl acetate obtained in August moved into the region of acetaldehyde, as shown in the PCA plots in Fig. 7.

A simple nonparametric algorithm (NPA) based on the Euclidean distance metric was used for comparison. In our experiments, the training set was adopted as the pattern templates and the Euclidean distances between testing samples and templates were calculated. The nearest neighbors are classified as one class. The same classification criteria were employed in the KIII application. Comparing the classification accuracy of the KIII and NPA (as shown in Table 2), we can find that the KIII network has better generalization capability.

4.4. Performance comparison with BP-NN

Usually, PARC selections are application-oriented and empirical. Some criteria, including high classification accuracy, fast, simple to train, low memory requirement, robust to outliers and to produce a measure of uncertainty, are proposed to attempt to determine the optimal classifier [38]. And several researchers have compared different PARCs employed by electronic noses [38,39]. To compare the performances, a conventional ANN, the back propagation trained neural network (BP-NN), as well as the KIII network, was applied to the classification. The BP-NN algorithm was taken from the neural network toolbox in MATLAB.

Being one of the most popular ANNs in electronic noses, BP-NN has become the de facto standard for pattern recognition of signals from a chemical sensor array. BP is a supervised learning algorithm based on the generalized delta rule, usually using gradient descent for minimizing the total squared output error between the desired and the actual net outputs. The performance of BP-NN is dependent on several factors, e.g., the number of hidden layers, learning rate, momentum and training data. More details can be referred to Ref. [40].

The BP-NN used in this paper is composed of 32 input nodes, 10 hidden nodes and six output nodes representing the clusters. The tan-sigmoid transfer function is selected for both the hidden and the output layers. A gradient descent with a learning ratio of 0.05 is chosen. To make fair comparison, both BP-NN and the KIII were trained using the same training set until both mean-squared errors reached the same order of magnitude. The neuron in BP-NN with the highest score in the output layer indicates which class the input sample belongs to. This tolerant classification criterion is similar to what used with the KIII. Five different runs were conducted for each trial to reduce the effect of the random initial weights in the training phase. The classification results of BP-NN are presented in Table 2 along with those of the KIII. The performance of BP-NN is not as good as the KIII under similar situation, although an optimization by trial and error may improve it quite a lot.

5. Conclusions

In this paper, a biologically inspired neural network, based on anatomical and electroencephalographic studies of biological olfactory systems, is applied to pattern recognition in electronic noses. Classifying six VOCs commonly presented in the headspace of Chinese rice wine, its performance to eliminate the concentration influence and counteract sensor drift is examined and compared with the simple nonparametric algorithm and the well-known BP-NN.

The KIII neural network has a good performance in classification of six VOCs of different concentrations, even for the patterns obtained 1 month later than what was used for training. Its flexibility and robust fault tolerance are quite suitable for electronic nose applications, subjecting to the problems associated with the susceptibility to concentration influence and sensor drift. Compared with BP-NN, the application of the KIII neural network is time-consuming and requires a lot of memory to solve lots of ODEs constructing the KIII; e.g., a 32-channel KIII network consists of over 200 ODEs. Although one classification performance required about 1 min in our experiments, it is fast enough to satisfy application requirement. Efficient numerical computation methods and DSP and VLSI hardware specially designed for parallel implementation are under research for other real-time applications.

The purpose of this paper is not to prove that the KIII network is superior to other techniques of signal processing in the electronic nose community. Instead, we just like to introduce a new method to process sensor array signals and to attract more researchers to pay attentions to this biological model of olfactory systems. Future works will be addressed on improving the performance of the KIII network in electronic nose application, especially fully utilizing the spatio-temporal dynamics properties of the model for time series signals from chemical sensor arrays. More biologically oriented learning and classification rules are still under investigation. We are sure that the study on electronic noses will help to understand signal processing in biological olfactory systems and vice versa.

Acknowledgements

References

[1] L. Buck, R. Axel, A novel multigene family may encode odorant receptors: a molecular basis for odor recognition, Cell 65 (1991) 175–187.

[2] J.W. Gardner, P.N. Bartlett, A brief history of electronic noses, Sensor Actuators B Chem. 18 (1994) 211–220.

[3] J.W. Gardner, P.N. Bartlett, Electronic Noses: Principles and Applications, Oxford University Press, New York, 1999.

[4] K.C. Persaud, P. Wareham, A.M. Pisanelli, E. Scorsone, Electronic nose—a new monitoring device for environmental applications, Sens. Mater. 17 (2005) 355–364.

[5] R.E. Baby, M. Cabezas, E.N. Walsöe de Reca, Electronic nose: a useful tool for monitoring environmental contamination, Sensor Actuators B Chem. 69 (2000) 214–218.

[6] M.P. Marti, R. Boqué, O. Busto, J. Guasch, Electronic noses in the quality control of alcoholic beverages, Trac-Trends Anal. Chem. 24 (2005) 57–66.

[7] S. Ampuero, J.O. Bosset, The electronic nose applied to dairy products: a review, Sensor Actuators B Chem. 94 (2003) 1–12.

[8] E. Schaller, J.O. Bosset, F. Escher, Electronic noses and their application to food, LWT-Food Sci. Technol. 31 (1998) 305–316.

[9] J.W. Gardner, H.W. Shin, E.L. Hines, An electronic nose system to diagnose illness, Sensor Actuators B Chem. 70 (2000) 19–24.

[10] J. Yinon, Detection of explosive by electronic noses, Anal. Chem. 75 (2003) 98A–105A.

[11] K.J. Albert, N.S. Lewis, C.L. Schauer, G.A. Sotzing, S.E. Stitzel, T.P. Vaid, D.R. Walt, Cross-reactive chemical sensor arrays, Chem. Rev. 100 (2000) 2595–2626.

[12] D. James, S.M. Scott, Z. Ali, W.T. O'Hare, Chemical sensors for electronic nose systems, Microchim. Acta 149 (2005) 1–17.

[13] E.L. Hines, E. Llobet, J.W. Gardner, Electronic noses: a review of signal processing techniques, IEE Proc. Circuit Device Syst. 146 (1999) 297–310.

[14] R. Gutierrez-Osuna, Pattern analysis for machine olfaction: a review, IEEE Sens. J. 2 (2002) 189–202.

[15] A.K. Srivastava, Detection of volatile organic compounds (VOCs) using SnO_2 gas-sensor array and artificial neural network, Sensor Actuators B Chem. 96 (2003) 24–37.

[16] M. Sriyudthsak, A. Teeramongkolrasasmee, T. Moriizumi, Radial basis neural networks for identification of volatile organic compounds, Sensor Actuators B Chem. 65 (2000) 358–360.

[17] M. Garcia, M. Aleixandre, J. Gutierrez, M.C. Horrillo, Electronic nose for wine discrimination, Sensor Actuators B Chem. 113 (2006) 911–916.

[18] C. Di Natale, A. Macagnano, A. D'Amico, F. Davide, Electronic-nose modeling and data analysis using a self-organizing map, Meas. Sci. Technol. 8 (1997) 1236–1243.

[19] Y. Yao, W.J. Freeman, Model of biological pattern recognition with spatially chaotic dynamics, Neural Netw. 3 (1990) 153–170.

[20] W.J. Freeman, Neurodynamics: An Exploration of Mesoscopic Brain Dynamics, Springer-Verlag, London, UK, 2000.

[21] H.J. Chang, W.J. Freeman, Parameter optimization in models of the olfactory neural system, Neural Netw. 9 (1996) 1–14.

[22] H.J. Chang, W.J. Freeman, B.C. Burke, Biologically modeled noise stabilizing neurodynamics for pattern recognition, Int. J. Bifurc. Chaos 8 (1998) 321–345.

[23] H.J. Chang, W.J. Freeman, B.C. Burke, Optimization of olfactory model in software to give 1/f power spectra reveals numerical instabilities in solutions governed by aperiodic (chaotic) attractors, Neural Netw. 11 (1998) 449–466.

[24] R. Kozma, W.J. Freeman, Chaotic resonance–methods and applications for robust classification of noise and variable patterns, Int. J. Bifurc. Chaos 11 (2001) 1607–1629.

[25] R. Kozma, W.J. Freeman, Classification of EEG patterns using nonlinear dynamics and identifying chaotic phase transitions, Neurocomputing 44–46 (2002) 1107–1112.

[26] X. Li, G. Li, L. Wang, W.J. Freeman, A study on a bionic pattern classifier based on olfactory neural system, Int. J. Bifurc. Chaos 16 (2006) 2425–2434.

[27] R. Gutierrez-Osuna, A. Gutierrez-Galvez, Habituation in the KIII olfactory model with chemical sensor arrays, IEEE Trans. Neural Netw. 14 (2003) 1565–1568.

[28] A. Gutierrez-Galvez, R. Gutierrez-Osuna, Increasing the separability of chemosensor array patterns with Hebbian/anti-Hebbian learning, Sensor Actuators B Chem. 116 (2006) 29–35.

[29] Z.D. Bao, R.N. Xu, Analysis of the flavor components in Yellow rice wine, Liquor Mak. 5 (1999) 65–67 (in Chinese).

[30] E. Llobet, J. Brezmes, X. Vilanova, J.E. Sueiras, X. Correig, Qualitative and quantitative analysis of volatile organic compounds using transient and steady-state responses of a thick-film tin oxide gas sensor array, Sensor Actuators B Chem. 41 (1997) 13–21.

[31] W.J. Freeman, Mass Action in the Nervous System, Academic Press, New York, 1975.

[32] W.J. Freeman, Simulation of chaotic EEG patterns with a dynamic model of the olfactory system, Biol. Cybern. 56 (1987) 139–150.

[33] W.J. Freeman, Nonlinear gain mediating cortical stimulus-response relations, Biol. Cybern. 33 (1979) 237–247.

[34] S. Quarder, U. Claussnitzer, M. Otto, Using singular-value decompositions to classify spatial patterns generated by a nonlinear dynamic model of the olfactory system, Chemometr. Intell. Lab. Syst. 59 (2001) 45–51.

[35] K. Shimoide, W.J. Freeman, Dynamic neural network derived from the olfactory system with examples of applications, IEICE Trans. Fundam. Electron. Commun. Comput. Sci. E78-A (1995) 869–884.

[36] M. Holmberg, F. Winquist, I. Lundström, F. Davide, C. Dinatale, A. D'Amico, Drift counteraction for an electronic nose, Sensor Actuators B Chem. 36 (1996) 528–535.

[37] T. Artursson, T. Eklöv, I. Lundström, P. Mårtensson, M. Sjöström, M. Holmberg, Drift correction for gas sensors using multivariate methods, J. Chemometr. 14 (2000) 711–723.

[38] R.E. Shaffer, S.L. Rose-Pehrsson, R.A. McGill, A comparison study of chemical sensor array pattern recognition algorithms, Anal. Chim. Acta 384 (1999) 305–317.

[39] M. Bicego, G. Tessari, G. Tecchiolli, M. Bettinelli, A comparative analysis of basic pattern recognition techniques for the development of small size electronic nose, Sensor Actuators B Chem. 85 (2002) 137–144.

[40] S. Haykin, Neural Networks: A Comprehensive Foundation, 2nd ed., Prentice-Hall, Englewood Cliffs, NJ, 1999.

Biographies

Jun Fu entered Zhejiang University, China in 1999, and received his BSc degree in biomedical engineering in 2004. Currently, he is a PhD candidate at Zhejiang University, majoring in biomedical engineering. His research interests include biosensors, pattern recognition and artificial olfaction.

Guang Li is a professor at the Department of Control Science and Engineering, Zhejiang University. He received his BSc and MSc Degrees in biomedical engineering at Zhejiang University, China in 1987 and 1991, respectively. He obtained his PhD degree in biomedical engineering at Imperial College of Science, Technology and Medicine, London, UK in 1998. He used to work at University of Glasgow and Moor Instruments Ltd., UK (1998–2001). His research interests include biosensors, biomedical instruments and neuroinformatics.

Yuqi Qin is a senior undergraduate student of biomedical engineering at Zhejiang University, China. She is also a member of Chu Kochen Hornor College of Zhejiang University. Her research interest is signal processing.

Walter J. Freeman studied physics and mathematics at M.I.T., philosophy at the University of Chicago, medicine at Yale University (M.D. cum laude 1954), internal medicine at Johns Hopkins, and neurophysiology at UCLA. He has taught brain science in the University of California at Berkeley since 1959, where he is Professor of the Graduate School. His research interests include nonlinear neurodynamics and brain science.